A ^{2}H Solid-State NMR Study of Lipid Clustering by Cationic Antimicrobial and Cell-Penetrating Peptides in Model Bacterial Membranes

Byungsu Kwon,[†] Alan J. Waring,[‡§] and Mei Hong[†*]
[†]Department of Chemistry, Iowa State University, Ames, Iowa; [‡]Department of Physiology and Biophysics, School of Medicine, University of California, Irvine, California; and [§]Department of Medicine, Harbor-UCLA Medical Center, Torrance California

ABSTRACT Domain formation in bacteria-mimetic membranes due to cationic peptide binding was recently proposed based on calorimetric data. We now use ^{2}H solid-state NMR to critically examine the presence and absence of domains in bacterial membranes containing zwitterionic 1-palmitoyl-2-oleoyl-*sn*-glycero-3-phosphatidylethanolamine (POPE) and anionic 1-palmitoyl-2-oleoyl-*sn*-glycero-3-phosphatidylglycerol (POPG) lipids. Chain-perdeuterated POPE and POPG are used in single-component membranes, binary POPE/POPG (3:1) membranes, and membranes containing one of four cationic peptides: two antimicrobial peptides (AMPs) of the β-hairpin family of protegrin-1 (PG-1), and two cell-penetrating peptides (CPPs), HIV TAT and penetratin. ^{2}H quadrupolar couplings were measured to determine the motional amplitudes of POPE and POPG acyl chains as a function of temperature. Homogeneously mixed POPE/POPG membranes should give the same quadrupolar couplings for the two lipids, whereas the presence of membrane domains enriched in one of the two lipids should cause distinct ^{2}H quadrupolar couplings that reflect different chain disorder. At physiological temperature (308 K), we observed no or only small coupling differences between POPE and POPG in the presence of any of the cationic peptides. However, around ambient temperature (293 K), at which gel- and liquid-crystalline phases coexist in the peptide-free POPE/POPG membrane, the peptides caused distinct quadrupolar couplings for the two lipids, indicating domain formation. The broad-spectrum antimicrobial peptide PG-1 ordered ~40% of the POPE lipids while disordering POPG. The Gram-negative selective PG-1 mutant, IB549, caused even larger differences in the POPE and POPG disorder: ~80% of POPE partitioned into the ordered phase, whereas all of the POPG remained in the disordered phase. In comparison, TAT rigidified POPE and POPG similarly in the binary membrane at ambient temperature, indicating that TAT does not cause dynamic heterogeneity but interacts with the membrane with a different mechanism. Penetratin maintained the POPE order but disordered POPG, suggesting moderate domain separation. These results provide insight into the extent of domain formation in bacterial membranes and the possible peptide structural requirements for this phenomenon.

INTRODUCTION

Lateral phase separation is well recognized for cholesterol- and sphingomyelin-rich lipid membranes that mimic the plasma membrane of eukaryotic cells (1,2). Recently, this domain formation was also proposed for model bacteria membranes containing both zwitterionic and anionic lipids (3). The proposal was based on the observation that bacteria-mimetic 1-palmitoyl-2-oleoyl-*sn*-glycero-3-phosphatidylethanolamine(POPE)/ 1-palmitoyl-2-oleoyl-*sn*-glycero-3-phosphatidylglycerol (POPG) and POPE/cardiolipin membranes containing certain cationic peptides show a phase transition at a high temperature that is similar to the transition temperature of the pure POPE membrane (4,5). In contrast, the phase transition of the peptide-free mixed membranes is broad and occurs at a lower temperature, which is intermediate between the transition temperatures of the two constituent lipids. These data led to the hypothesis that cationic peptides sequester anionic lipids, so that the zwitterionic POPE is segregated into a single-component domain whose physical chemical property is similar to that of the pure POPE membrane. It was further proposed that this charge clustering and domain formation may explain the Gram-selective activity of some cationic antimicrobial peptides (AMPs): Gram-negative bacteria such as *Escherichia coli* contain significant amounts of both zwitterionic and anionic lipids in their cytoplasmic membranes, whereas the membranes of many Gram-positive bacteria such as *Staphylococcus aureus* contain predominantly anionic lipids such as POPG and cardiolipin, and therefore cannot form domains (6). This domain formation does not appear to be ubiquitous for all cationic membrane peptides: peptides that cluster anionic lipids appear to have the common features of a high density of positive charges and conformational flexibility, although the number of characterized lipid-clustering peptides is still small.

Indirect evidence of domain formation in model bacterial membranes has also been reported based on small-angle x-ray scattering (SAXS) experiments of POPE-rich membranes containing cationic peptides such as antimicrobial defensins and cell-penetrating peptides (CPPs) such as HIV TAT. When the molar ratios of phosphatidylethanolamine (PE) and anionic lipids are comparable to the bacterial membrane composition, which contains 20–30% anionic lipids, saddle-splay or negative Gaussian curvature was observed (7,8). This Gaussian curvature generation was proposed to be important for membrane processes

Submitted June 1, 2013, and accepted for publication August 19, 2013.

*Correspondence: mhong@iastate.edu

Editor: Klaus Gawrisch.

0006-3495/13/11/2333/10 $2.00

http://dx.doi.org/10.1016/j.bpj.2013.08.020

such as pore formation, blebbing, and vesicularization (7). Lower PE content weakens the negative Gaussian curvature, suggesting that the cationic peptides may cause PE enrichment in these model bacterial membranes.

Elucidating the lipid interactions of cationic peptides is important for understanding the structural basis for the actions of AMPs and CPPs (9,10). These Arg-rich peptides share similar amino acid sequences but distinct biological activities. AMPs constitute the primary line of defense by the innate immune system of many multicellular organisms (11,12). They disrupt the barrier function of the lipid membranes of microbial cells by forming membrane pores or by micellizing the lipid membrane. In contrast, CPPs can cross the membrane into cells without damaging the cell membrane, and can do so while carrying macromolecular cargos (13). Although most AMPs are amphipathic molecules with well-defined structures, solid-state NMR (SSNMR) studies showed that two prototypical CPPs, HIV TAT and penetratin, are highly mobile and are both unstructured or low in strand and helix content in the lipid membrane (14,15). This conformational flexibility was proposed to underlie the rapid translocation of CPPs across the lipid membrane, without being stuck in the membrane to cause long-lasting defects (9). NMR distance measurements and two-dimensional correlation spectra showed that Arg-phosphate interactions and Arg-water interactions are common in both AMPs and CPPs (15–17) to stabilize the positive charges in the hydrophobic part of the lipid membrane.

In this work, we use ^{2}H SSNMR to investigate whether membrane domains are induced by four cationic AMPs and CPPs, to test the hypothesis that lipid clustering may be one of the mechanisms of action of these peptides. We investigate whether lipid domains that are stable on the millisecond timescale or longer and that are larger than ~30 nm exist in the model bacterial membrane, POPE/POPG (3:1). We measure acyl-chain ^{2}H quadrupolar couplings, which reflect the C-H order parameters of POPE and POPG in the binary membrane in the absence and presence of the peptides. If membrane domains are induced by the peptides, the quadrupolar couplings of the lipids in the peptide-poor domain should approach the couplings of the corresponding single-component membrane, and we can quantify the distribution of each lipid in the different domains by simulating ^{2}H spectra as a superposition of basis spectra extracted from limiting conditions.

Four cationic peptides are chosen for this study. The β-hairpin AMP protegrin-1 (PG-1) has been extensively studied using SSNMR (9,10) and molecular dynamics simulations (18,19). This 18-residue hexa-Arg peptide forms oligomeric transmembrane β-barrels in POPE/POPG (3:1) membranes (20,21). It has nonselective antimicrobial activities against both Gram-negative and Gram-positive bacteria, with minimum effective concentrations in the 1–2 μg/ml range (22). The second peptide is a PG-1 mutant, IB549, in which all six Arg residues have been replaced by Lys. IB549 is selective against Gram-negative bacteria: it is about twofold more potent than PG-1 against Gram-negative *Pseudomonas aeruginosa* but 32-fold less active than PG-1 against Gram-positive methicillin-resistant *S. aureus* (23). Thus, IB549 is a good candidate for investigating whether lipid clustering is correlated with Gram selectivity of AMPs. We also studied two cell-penetrating peptides, HIV TAT and penetratin. The 15-residue TAT peptide contains 6 Args and 2 Lys residues in a contiguous stretch. This highly charged peptide is a random coil in lipid membranes (15) and generates negative Gaussian curvature based on SAXS data (7). For comparison, the CPP penetratin is less mobile and contains β-turns interspersed with short segments of β-strands (14). We show that these conformationally and dynamically distinct peptides do not induce large and stable lipid domains at physiological temperature, but at ambient temperature, the two AMPs indeed induce membrane domains enriched in one of the two lipids.

MATERIALS AND METHODS

Membrane sample preparation

POPE, POPG, 1-palmitoyl (d_{31})-2-oleoyl-*sn*-glycero-3-phosphoethanolamine (d_{31}-POPE), and 1-palmitoyl (d_{31})-2-oleoyl-*sn*-glycero-3-[phospho-*rac*-(1-glycerol)] (sodium salt) (d_{31}-POPG) were purchased from Avanti Polar Lipids (Alabaster, AL). All peptides were synthesized by Fmoc solid-phase peptide synthesis protocol and purified by HPLC to >95% purity. The amino acid sequences are PG-1 (NH_2-RGGRLCYCRRRFC VCVGR-$CONH_2$), IB549 (NH_2-KGGKLCYCKKKFCVCVGK-COOH), TAT(48–60) (GRKKRRQRRRPPQ-$CONH_2$), and penetratin (RQIKIWFQ NRR-MKWKK-$CONH_2$).

POPE, POPG, and POPE/POPG (3:1) membranes were prepared by dissolving the lipids in chloroform/methanol (1:1) solution, dried under nitrogen gas, redissolved in cyclohexane, and lyophilized overnight. The dry and homogeneous lipid powder was dissolved in 2.5 mL Tris buffer (10 mM, pH 7.5) and freeze-thawed 10 times to obtain uniform vesicles. The peptide was dissolved in 0.5 mL Tris buffer and mixed with the lipid vesicle solutions. Peptide-lipid mixing caused immediate and significant precipitation, indicating strong binding of the peptides to the lipids. The solution was incubated overnight at room temperature, and then centrifuged at 55,000 rpm and 4°C for ~6 h to obtain a homogeneous membrane pellet. The pellet was spun down into a pipette tip, air-dried to a hydration level of 35–40%, and then spun into a 4 mm magic-angle-spinning rotor. All membrane samples were hydrated with regular water containing deuterium spins at their natural abundance of 0.01%. The lack of an isotropic peak in all peptide-free membrane spectra confirms that at the hydration level used, the amount of natural abundance deuterated water was below the detection limit. The peptide/lipid molar ratio was 1:15 for all samples.

SSNMR experiments

All SSNMR spectra were measured on a wide-bore Bruker AVANCE 600 MHz (14.1 T) spectrometer operating at 600.13 MHz and 92.12 MHz for ^{1}H and ^{2}H, respectively. A 4 mm magic-angle-spinning probe was used in the static mode for all ^{2}H experiments. ^{2}H spectra were measured from 308 to 283 K. Sample temperatures were direct readings from the thermocouple positioned near the sample cavity and are estimated to be within 1 K of the true temperature for these static experiments. All samples were stabilized at the desired temperature for at least 1 hour before the spectrum was recorded. ^{2}H quadrupolar echo spectra were measured using echo

delays of 40 and 32 μs before and after the second 90° pulse, a ^{2}H 90° pulse length of 5 μs, a recycle delay of 0.5 s, and a spectral width of 500 kHz. Suitable left shift was applied before Fourier transformation to obtain a flat baseline for all spectra.

Spectral deconvolution

Ambient-temperature ^{2}H spectra of d_{31}-POPE and d_{31}-POPG of the POPE/POPG membrane were deconvolved to obtain the relative amounts of each lipid in the gel phase and the liquid-crystalline (LC) phase. For this deconvolution, the 308 K spectrum and the 283 K spectrum of the peptide-free POPE/POPG membrane were used as the basis spectra to represent the LC phase and the gel phase, respectively.

RESULTS

^{2}H spectra of d_{31}-POPE and d_{31}-POPG at 308 K

We use ^{2}H quadrupolar couplings of d_{31}-POPE and d_{31}-POPG to probe whether the anionic POPG is clustered by the cationic peptides to form a separate domain from POPE. ^{2}H quadrupolar couplings reflect the time-averaged orientations of the C-H bonds relative to the bilayer normal. Large-amplitude motions of disordered lipids lead to small ^{2}H quadrupolar couplings, i.e., small C-H order parameters. If POPE and POPG are homogeneously mixed on the nanometer scale, they should then exhibit similar quadrupolar couplings; moreover, these couplings should be intermediate between the values of each lipid in its own single-component membrane. The gel-to-LC phase transition temperatures (T_m) of undeuterated POPE and POPG are 298 and 271 K, respectively. Deuteration decreases the T_m by a few degrees, as confirmed experimentally below. Thus, at a given temperature, the pure POPE membrane has larger couplings than the pure POPG membrane (Fig. 1 *a*) due to the higher order of POPE lipids. If membrane domains enriched in one of the two lipids are present, the corresponding quadrupolar couplings should then revert to or approach the couplings of the single-component membrane at that temperature. We first show ^{2}H spectra measured at 308 K, near physiological temperature, and then describe the ^{2}H spectra at lower temperatures of 298–283 K.

Fig. 1 shows the 308 K ^{2}H spectra of d_{31}-POPE and d_{31}-POPG in single- and two-component membranes without and with PG-1 and TAT. Four sets of samples are compared: the one-component POPE and POPG membranes, the peptide-bound one-component membranes, the peptide-free POPE/POPG membrane, and the peptide-bound POPE/POPG membrane. Each spectrum is a superposition of the symmetric Pake patterns of all the methylene and methyl groups along the palmitoyl chain. The ^{2}H spectra of the single-component membranes reflect the order parameter distribution along the acyl chain when all lipid molecules undergo the same motions. For simplicity, we use the maximum ^{2}H quadrupolar coupling, read off from the outermost 90° edges of the spectra, to represent the overall

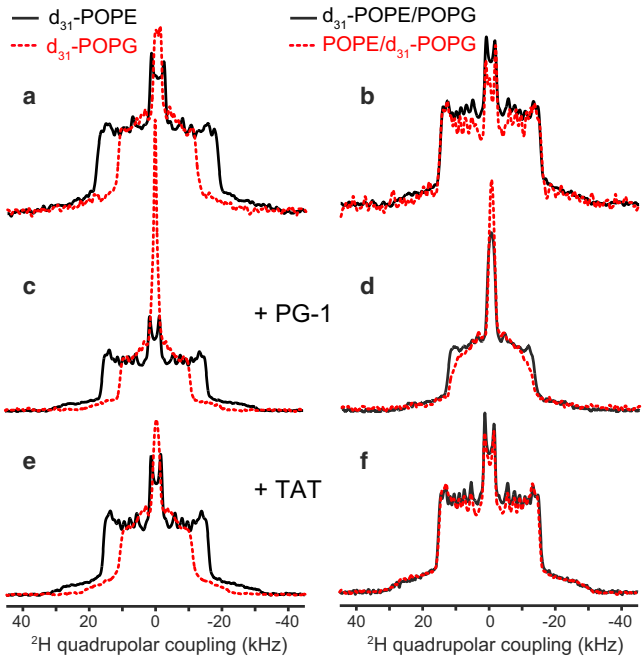

FIGURE 1 308 K ^{2}H spectra of d_{31}-POPE (*solid lines*) and d_{31}-POPG (*dashed lines*) in various lipid membranes. (*a*) Single-component POPE membrane and POPG membrane. The couplings of the two lipids differ significantly, indicating different motional amplitudes of POPE and POPG at this temperature. (*b*) POPE/POPG (3:1) membrane. The two lipids exhibit the same quadrupolar couplings, indicating homogeneous mixing. (*c*) PG-1-bound POPE membrane and POPG membrane, showing different couplings that are smaller than the corresponding peptide-free single-component membrane. (*d*) PG-1-bound POPE/POPG membrane, showing similar couplings for POPE and POPG, indicating homogeneous mixing of the two lipids. (*e*) TAT-bound POPE membrane and POPG membrane. (*f*) TAT-bound POPE/POPG membrane, where the couplings of the two lipids are unchanged from the peptide-free membrane. To see this figure in color, go online.

motional amplitude of the lipids (Table 1). This maximum coupling results from the C2 methylene group at the beginning of the palmitoyl chain, which is the most conformationally restricted segment in the acyl chain due to its proximity to the glycerol backbone (24,25). The smallest splitting in these ^{2}H spectra results from the methyl group

TABLE 1 Maximum ^{2}H quadrupolar couplings (kHz) of lipid membranes in the absence and presence of cationic membrane peptides at 308 K

d_{31}-POPE		d_{31}-POPG	
d_{31}-POPE	36.6	d_{31}-POPG	23.6
d_{31}-POPE + PG-1	31.5	d_{31}-POPG + PG-1	21.1
d_{31}-POPE + TAT	31.7	d_{31}-POPG + TAT	21.7
d_{31}-POPE + IB549	31.8	d_{31}-POPG + IB549	20.8
d_{31}-POPE + penetratin	31.6	d_{31}-POPG + penetratin	20.2
d_{31}-POPE/POPG	30.3	POPE/d_{31}-POPG	30.7
d_{31}-POPE/POPG + PG-1	25.8	POPE/d_{31}-POPG + PG-1	24.4
d_{31}-POPE/POPG + TAT	30.9	POPE/d_{31}-POPG + TAT	30.3
d_{31}-POPE/POPG + IB549	26.9	POPE/d_{31}-POPG + IB549	24.6
d_{31}-POPE/POPG + penetratin	26.9	POPE/d_{31}-POPG + penetratin	26.2

at the end of the acyl chain. In most spectra shown here, the maximum and minimum quadrupolar couplings correlate: larger C2 quadrupolar coupling is associated with larger methyl splitting. No dePaking (26,27) was attempted because the spectra of many peptide-bound membranes do not have sufficient resolution, which may partly result from the presence of intermediate-timescale motion of the acyl chains.

In the absence of any peptide, the pure POPE membrane exhibited a maximum quadrupolar coupling of 36.6 kHz at 308 K. Adding POPG to 25 mol % reduced the POPE couplings significantly, to a maximum value of 30.3 kHz (Fig. 1, *a* and *b*), indicating that the low-melting POPG increased the disorder of the high-melting POPE. PG-1 binding to the POPE membrane similarly reduced the maximum coupling to 31.5 kHz (Fig. 1 *c*), indicating that PG-1 exerted a similar disordering effect as POPG. PG-1 binding to the POPE/POPG membrane reduced the POPE quadrupolar couplings further, to 25.8 kHz (Fig. 1 *d*). Thus, instead of promoting a more ordered POPE-rich domain with couplings approaching that of the pure POPE membrane, PG-1 increased the POPE disorder, thus ruling out a POPE-rich domain at 308 K.

Compared to POPE, the single-component POPG membrane shows much smaller quadrupolar couplings at 308 K, with a maximum value 23.6 kHz. Mixing with POPE increased the POPG couplings to the same values as the POPE couplings in the binary membrane (Fig. 1 *b*), indicating unambiguously that the two lipids are homogeneously mixed and exist in a single LC phase at this temperature. PG-1 binding to the POPG membrane moderately decreased the quadrupolar couplings (maximum value 21.1 kHz) compared to the peptide-free POPG membrane. In contrast, PG-1 binding to the POPE/POPG membrane caused a maximum POPG coupling of 24.4 kHz, which is smaller than the coupling of the peptide-free POPE/POPG membrane but higher than the couplings of the POPG membrane with or without PG-1. Instead, the 24.4 kHz coupling is similar to the maximum POPE coupling in the same peptide-bound binary membrane, indicating that PG-1 largely maintained the homogeneous mixing of the two lipids. Therefore, the PG-1-bound POPE/POPG membrane does not show any significant domain formation at 308 K.

TAT shows very different lipid interactions from PG-1 at 308 K. The POPE quadrupolar couplings are similar (~31 kHz) for TAT-bound d_{31}-POPE membrane, peptide-free d_{31}-POPE/POPG membrane, and TAT-bound d_{31}-POPE/POPG membrane (Fig. 1, *b*, *e*, and *f*), indicating that TAT behaves identically to POPG in causing disorder to POPE. In addition, TAT-bound POPG membrane has similar couplings as the pure d_{31}-POPG membrane, and TAT-bound POPE/d_{31}-POPG membrane has similar couplings as the peptide-free POPE/d_{31}-POPG membrane. Taken together, these results indicate that TAT does not perturb either the POPE or POPG dynamics in any of these membranes at 308 K.

These ^{2}H spectra indicate the following lipid mixing situations at 308 K. In the absence of peptides, the POPE/POPG membrane is homogeneously mixed, with similar quadrupolar couplings that differ from the individual lipid's couplings in its own membrane (see the Supporting Material, Fig. S1 *a*). Binding of PG-1 and TAT to single-component membranes reduced the POPE couplings significantly and the POPG couplings moderately. Thus, both PG-1 and TAT increased the disorder of the single-component membranes. For the POPE/POPG membrane, PG-1 binding caused similar quadrupolar couplings (24–26 kHz) for the two lipids, both of which are much smaller than the couplings of the peptide-free POPE/POPG membranes. Therefore, PG-1 increased the disorder of both lipids in the binary membrane but did not cause domain separation. TAT also induced similar disorder to POPE and POPG in the binary membrane, but the couplings are unchanged from the peptide-free membranes (Fig. S1 *b*), thus TAT does not change the membrane disorder at all, in contrast to PG-1.

The ^{2}H spectra of d_{31}-POPG in PG-1-bound membranes and TAT-bound POPG membrane show a pronounced isotropic peak (Fig. 1, *c–e*). These isotropic peaks are only observed when the rest of the palmitoyl chain shows much weaker couplings, and the intensity envelope excluding the isotropic peak is also higher in the middle of these spectra. These features indicate that the isotropic peak results from the chain-end methyl group, which becomes more disordered after peptide binding, therefore the methyl splitting is no longer resolved but merges into a single narrow peak.

To investigate how general these peptide-lipid interactions are, we also measured the ^{2}H spectra of IB549 and penetratin at 308 K (Fig. 2). IB549 gave rise to similar ^{2}H spectra as PG-1: it caused similar but not identical maximum quadrupolar couplings for POPE (26.9 kHz) and POPG (24.6 kHz) (Fig. 2 *b*). Penetratin behaves in an intermediate regime between PG-1 and TAT: it caused the same quadrupolar couplings for POPE and POPG in the binary membrane, but both couplings are much smaller than the values of the peptide-free membrane (Fig. 2 *d*, Table 1). Fig. S1 summarizes the maximum quadrupolar couplings of POPE and POPG of the various lipid membranes at 308 K.

Ambient-temperature ^{2}H spectra of peptide-free lipid membranes

Because lipid motion and membrane disorder depend intimately on temperature, we measured the ^{2}H spectra of the POPE/POPG membrane at lower temperatures of 298 to 283 K. We first describe the ^{2}H spectra of peptide-free membranes at these temperatures. The spectra of the pure POPE membrane (Fig. S2, *c–e*) are clearly broadened below 293 K, consistent with phase transition of POPE at 298 K.

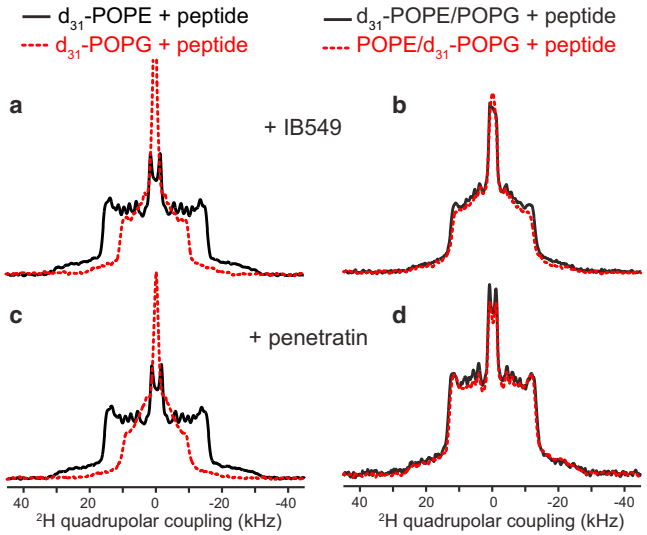

FIGURE 2 308 K ^{2}H spectra of d_{31}-POPE (*solid lines*) and d_{31}-POPG (*dashed lines*) in various peptide-containing lipid membranes. (*a*) IB549-containing POPE membrane and POPG membrane. The two lipids show very different couplings or motional amplitudes. (*b*) IB549-bound POPE/POPG membranes, showing the same couplings for the two lipids, indicating an absence of lateral domains. (*c*) Penetratin-bound POPE membrane and POPG membrane. (*d*) Penetratin-bound POPE/POPG membrane, showing the same couplings for the two lipids, indicating an absence of lateral domains. To see this figure in color, go online.

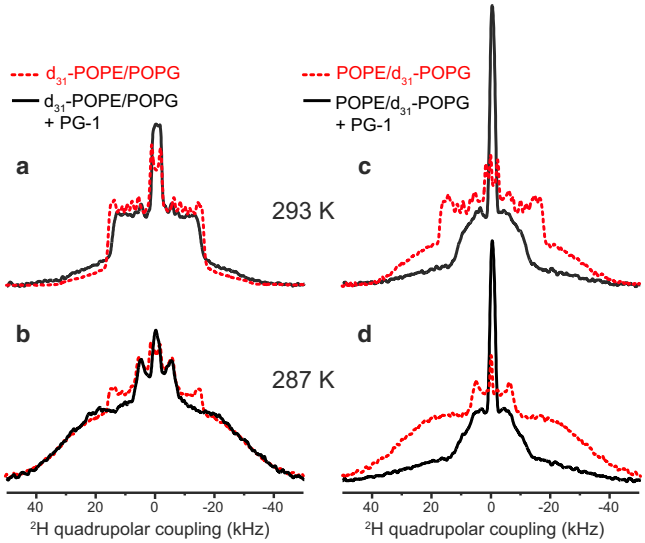

FIGURE 3 Effect of PG-1 on the POPE/POPG membranes at 293 and 287 K. ^{2}H spectra without PG-1 are shown in dashed lines and with PG-1 are shown in solid lines. (*a*) d_{31}-POPE/POPG membrane at 293 K. POPE is predominantly (82%) in the LC phase in the absence of peptide and acquires significant (40%) gel-phase content upon PG-1 binding. (*b*) d_{31}-POPE/POPG membrane at 287 K. POPE is predominantly in the gel phase in both cases. (*c*) POPE/d_{31}-POPG spectrum at 293 K. POPG is ~62% in the gel phase without PG-1 but becomes mostly disordered in the presence of PG-1. (*d*) 287 K spectra of POPE/d_{31}-POPG. POPG is predominantly in the gel phase in the absence of peptide and becomes mostly fluid upon PG-1 binding. To see this figure in color, go online.

For the POPE/POPG membrane, the d_{31}-POPE spectra at 293 and 287 K are a superposition of LC- and gel-phase spectra (Fig. 3, *a* and *b*).

We quantified the percentages of POPE in the LC and gel phases by simulating the spectra as a superposition of the 308 K spectrum and the 283 K spectrum of the peptide-free POPE/POPG membrane (Fig. 4). The superposition shows that for the 287 K binary membrane, POPE is distributed in the LC and gel phases at a 16%:84% ($\pm$2%) ratio. Increasing the temperature by only a few degrees, to 293 K, inverted the relative LC and gel phase concentrations to 82% for the LC phase and 18% for the gel phase. Thus, POPE partitioning between the LC and gel phases is highly sensitive to temperature in this narrow range. These observations are quantitatively consistent with the known phase diagram of the POPE/POPG membrane (28), which was assembled based on DSC, x-ray scattering, and optical microscopy data. The phase diagram indicates a coexistence temperature range of 291–296 K for a POPG mole fraction of 25%. At 293 K, the phase diagram indicates that the LC- and gel-phase concentrations are 29% and 71% ($\pm$2%), respectively, and ~75% of POPE is enriched in the gel phase, whereas POPG distribution is 40%:60% between the LC phase and the gel phase, respectively. The ^{2}H-NMR determined POPE distribution in the two phases at 287 K is roughly consistent with the predicted phase composition at 293 K, although the 293 K ^{2}H spectrum of POPE is roughly consistent with the 295 K phase composition. The small temperature shift between the ^{2}H NMR results and the x-ray and calorimetry-deduced phase diagram likely results from the well-known reduction of the phase transition temperature by lipid chain perdeuteration (29,30).

The d_{31}-POPG couplings between 293 and 287 K differ slightly (~3 kHz for the maximum coupling) from the couplings at 308 K (Fig. S2). If we neglect this difference, the 293 K d_{31}-POPG spectrum of the POPE/POPG membrane then corresponds to a superposition of 38% LC phase and 62% gel phase, which is in excellent agreement with the phase-diagram prediction of POPG distribution in the two phases (28).

Ambient-temperature ^{2}H spectra of peptide-bound POPE/POPG membranes

The effects of PG-1 and IB549 binding on the lipid mobility of the binary membranes at ambient temperatures are shown in Fig. 3 and Fig. 5. In contrast to the 308 K situation, PG-1 and IB549 changed the POPE and POPG couplings in opposite directions, indicating lipid clustering and domain formation. At 293 and 287 K (Fig. 3), PG-1 increased the gel-phase intensities of d_{31}-POPE while decreasing the gel-phase contribution of the d_{31}-POPG spectra. The gel-phase fraction of POPE at 293 K is 40%,

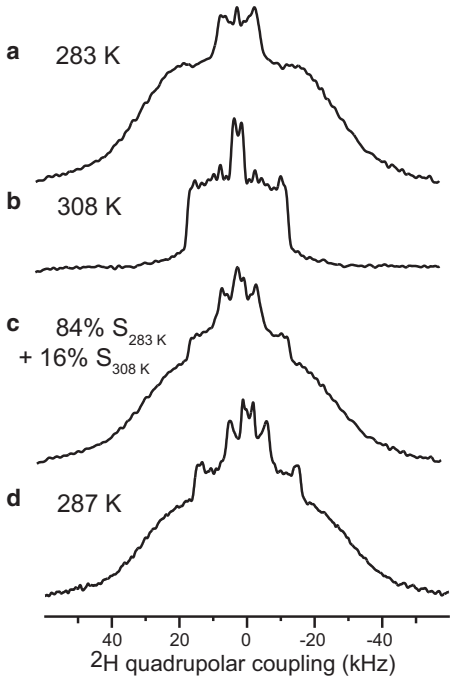

FIGURE 4 Extraction of the relative concentrations of POPE in the ordered and disordered phases. (*a*) 283 K ^{2}H spectrum of the d_{31}-POPE/POPG membrane. (*b*) 308 K ^{2}H spectrum of the d_{31}-POPE/POPG membrane. (*c*) Sum of the 283 and 308 K spectra with an 84%/16% ratio of the integrated intensities. (*d*) Measured 287 K ^{2}H spectrum of d_{31}-POPE/POPG, showing good agreement with (*c*).

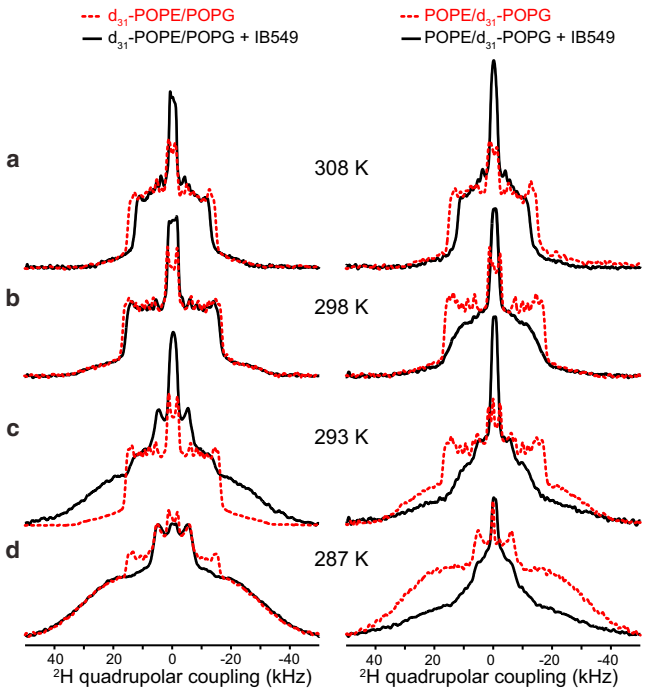

FIGURE 5 Influence of IB549 on POPE/POPG membrane, observed from the ^{2}H spectra at (*a*) 308 K, (*b*) 298 K, (*c*) 293 K, and (*d*) 287 K. Spectra of the peptide-free membranes are shown in dashed lines and the peptide-bound membranes are shown in solid lines. Left column: d_{31}-POPE/POPG. Right column: POPE/d_{31}-POPG. At 293 K, POPE becomes much more ordered in the presence of IB549, whereas POPG remains disordered. At 287 K, POPE is mainly in the ordered phase with or without the peptide, but POPG is much more disordered in the presence of IB549 than in its absence. To see this figure in color, go online.

up from 18% for the peptide-free binary membrane, although at 287 K, the gel-phase fraction of POPE increased from 84% to 96% (Table 2). Thus, PG-1 increased the order of POPE while increasing the disorder of POPG, indicating that POPE and POPG are preferentially separated. IB549 increased the rigidity of POPE even more strongly than PG-1 while maintaining the POPG disorder (Fig. 5): the gel-phase fraction of POPE is 83% at 293 K, almost twice the amount for the PG-1-bound binary membrane.

Compared to the two AMPs, TAT affected the POPE/POPG membrane qualitatively differently (Fig. 6): between 298 and 287 K, both POPE and POPG became more ordered in the presence of TAT. Spectral deconvolution indicates that the gel-phase fraction of each lipid is within 5–15% of each other in this temperature range (Table 2). Thus, TAT uniformly increased the order of both lipids instead of causing dynamically different membrane domains. Interestingly, penetratin, although also classified as a CPP, differs from TAT in its interaction with the lipids. Between 293 and 287 K, penetratin caused little change to the POPE disorder (Fig. S3, Table 2) but significantly increased the POPG disorder (smaller quadrupolar couplings). Thus, penetratin interaction with POPE and POPG is intermediate between the behaviors of the AMPs and TAT.

DISCUSSION

Although domain formation has been extensively studied in cholesterol-containing synthetic membranes that mimic the eukaryotic membrane (31,32), domain formation in bacterial membranes is a relatively recent proposal (3). ^{2}H NMR is an excellent probe of the dynamic heterogeneity of lipid membranes and has been used to study the phase diagram of ternary membranes containing cholesterol (33,34). For the model bacterial membrane studied here, if zwitterionic POPE and anionic POPG are separated into sufficiently large lateral domains with different chain mobilities, the quadrupolar couplings of the two lipids should then differ and should approach the values of their single-component membranes (Fig. 1 *a*). If, however, the domains are small or transient, lateral diffusion of the lipids between the domains will then average the quadrupolar couplings. For a maximum ^{2}H quadrupolar coupling of 20–30 kHz, chemical exchange on the timescale of ~50 μs or shorter will give fast-averaged spectra. Assuming a lipid lateral diffusion coefficient D_L of 5×10^{-8} cm^2/s, this timescale translates to a domain radius (r) of ~30 nm based on the diffusion equation $\langle r^2 \rangle = 4D_L\tau_c$. The domains must be smaller than ~30 nm to observe averaged quadrupolar

TABLE 2 Mole fractions of d_{31}-POPE and d_{31}-POPG in the disordered and ordered phases of the POPE/POPG membrane from 298 to 287 K, obtained from deconvolution of the ^{2}H NMR spectra

Temperature	Membrane	Disordered phase	Ordered Phase
298 K	d_{31}-POPE/POPG	~100%	~0%
	d_{31}-POPE/POPG + TAT	65%	35%
	POPE/d_{31}-POPG	~100%	~0%
	POPE/d_{31}-POPG + TAT	50%	50%
295 K	d_{31}-POPE/POPG	~100%	~0%
	d_{31}-POPE/POPG + TAT	23%	77%
	POPE/d_{31}-POPG	~100%	~0%
	POPE/d_{31}-POPG + TAT	21%	79%
293 K	d_{31}-POPE/POPG	82%	18%
	d_{31}-POPE/POPG + PG-1	60%	40%
	d_{31}-POPE/POPG + IB549	17%	83%
	d_{31}-POPE/POPG + TAT	~0%	~100%
	d_{31}-POPE/POPG + penetratin	82%	18%
	POPE/d_{31}-POPG	38%	62%
	POPE/d_{31}-POPG + PG-1	~100%	~0%
	POPE/d_{31}-POPG + TAT	7%	93%
	POPE/d_{31}-POPG + penetratin	71%	29%
287 K	d_{31}-POPE/POPG	16%	84%
	d_{31}-POPE/POPG + PG-1	4%	96%
	d_{31}-POPE/POPG + IB549	4%	96%
	d_{31}-POPE/POPG + TAT	~0%	~100%
	d_{31}-POPE/POPG + penetratin	5%	95%
	POPE/d_{31}-POPG	~0%	~100%
	POPE/d_{31}-POPG + penetratin	8%	92%

couplings between the two domains. In other words, if different quadrupolar couplings are observed for the two domains, the domains must be much larger than ~30 nm. Although this size estimate depends on the value of D_L, diffusion coefficients in general differ by less than an order of magnitude among divergent lipid membranes. When the two domains are a gel phase and a fluid phase with different D_L values, which can in principle slow down lipid diffusion across the phase boundary, the domain size still cannot be much smaller than several tens of nanometers, because dynamic differences and diffusion coefficient contrasts cannot be maintained across very small domains. Indeed, experimental evidence suggests that the coexistence of multiple phases in a membrane does not cause significant changes of the diffusion coefficients for domain sizes $<$ ~200 nm (35), and the low diffusion coefficients measured for gel-phase lipids came from micron-sized membrane domains (36).

The ^{2}H NMR spectra shown here indicate that near the human physiological temperature of 308 K, the two AMPs caused very similar but not identical quadrupolar couplings for POPE and POPG, whereas the two CPPs induced identical couplings for the two lipids in the binary membrane (Figs. 1 and 2). The POPE couplings in the binary membrane are 6–10 kHz smaller than the couplings of the pure POPE membrane and the peptide-bound POPE membrane (Table 1), indicating the absence of a large POPE-enriched domain at 308 K. For PG-1 and IB549, the maximum quadrupolar couplings are 1.4 and 2.3 kHz larger for POPE than POPG. These differences are larger than the 0.4 kHz difference for the peptide-free binary membrane, suggesting that the two AMPs cause a small degree of domain separation. However, the main conclusion at 308 K is that the four cationic peptides induce either no or very minor domain separation in the POPE/POPG membrane.

The fact that the two AMPs increased the disorder of POPE and POPG at 308 K is consistent with the membrane-disruptive effect of these β-hairpin AMPs. HIV TAT did not affect the membrane disorder, which is consistent with its random coil nature (15). In comparison, penetratin increased the membrane disorder, similar to the two AMPs. This may be attributed to the fact that penetratin, unlike TAT, shows β-turn and short β-strand conformations (14,37), and the presence of such H-bonded conformations may facilitate the creation of membrane disorder.

The domain phenomenon changes completely at ambient temperatures of 293–287 K. Both AMPs increased the order of POPE while disordering POPG. Spectral deconvolution indicates that LC and gel phases coexist in this temperature range for the peptide-free POPE/POPG membrane, with the two lipids partitioning into the two phases according to the phase diagram: POPE has only a small gel-phase content (18%) at 293 K but becomes predominantly gel phase at 287 K, whereas POPG is ~60% gel phase at 293 K but 100% gel phase at 287 K (Table 2). PG-1 binding increased the gel-phase content of POPE to 40% at 293 K while keeping POPG predominantly disordered. Thus, PG-1 induced membrane domains at these ambient temperatures: the disordered domain contains a mixture of POPE and POPG, whereas the ordered domain consists exclusively of POPE. Relative to the total lipid content, in the PG-1-bound POPE/POPG membrane, all 25% POPG and 45% POPE reside in the disordered phase, whereas the remaining 30% POPE is separated into the gel phase. A POPE gel phase may not be directly involved in pore formation, because the ordered acyl chains should reduce the negative curvature strain of this lipid compared to the LC phase. However, the existence of significant gel phase may inhibit the function of biological membranes in other ways, for example by impeding protein lateral diffusion.

The Gram-negative-selective AMP, IB549, caused even stronger counter-directional changes to the POPE and POPG chain dynamics. At 293 K the gel-phase content of POPE increased to 83% (Fig. 5, Table 2), which is double that of the PG-1-bound membrane, whereas POPG remained similarly disordered as before. The ^{2}H spectra of the POPE/d_{31}-POPG membrane in the presence of both IB549 and PG-1 show modestly smaller couplings (Fig. 3 *c*, Fig. 5 *c*) compared to the high-temperature spectra of the peptide-free membranes, thus exact deconvolution is not possible. However, the small quadrupolar couplings qualitatively indicate the high disorder of POPG, consistent

with the notion that POPG preferentially interacts with IB549 and PG-1. Taken together, these data indicate that the Gram-negative antimicrobial activity of IB549 is indeed correlated with its stronger lipid-clustering ability. The structural cause for this stronger lipid clustering may be that the Lys ammonium group, due to its three-site jump motion, is less able to form stable H-bonds with lipid phosphate groups, thus it may predominantly interact with the anionic POPG. In contrast, the Arg variant of AMPs can interact with both POPG and POPE well, thus causing less domain separation.

Compared to the two AMPs, TAT affected the order of the binary membrane differently at ambient temperatures. It increased the gel-phase fraction of both POPE and POPG (Fig. 6), and the gel phase appeared at higher temperatures (298 K) than PG-1- and IB549-bound membranes. Thus, although TAT showed almost no effect to the membrane fluidity at 308 K, it exerted a uniform ordering effect on the binary membrane below 298 K, without causing domains. The molecular mechanism for this uniform ordering is still unclear. A hypothesis proposed by Wong and co-workers (7) based on SAXS data of CPPs is that the conformationally flexible and Arg-rich CPPs can efficiently cross-link multiple lipid headgroups through multidentate hydrogen bonds between the Arg guanidinium and lipid phosphate groups. In principle, this mechanism should not distinguish between POPE and POPG, and hence may explain the similar rigidification of both lipids. Direct distance measurement between Arg and phosphates by SSNMR showed the existence of short guanidinium-phosphate distances in many Arg-rich cationic peptides (9,15,17,37–39), although these data did not directly indicate the number of phosphate groups bound to each guanidinium. The second CPP, penetratin, interacts with the lipids in a more analogous fashion to the two AMPs: it enhanced the dynamic disorder of POPG while exerting relatively weak effects on the POPE order, suggesting that the penetratin-bound membrane may have moderate separation of POPE and POPG.

Taken together, these ^{2}H NMR data indicate that lipid clustering in the model bacterial membrane is a partial phenomenon that occurs within a narrow temperature range. This temperature range is well below the human physiological temperature but is near the temperature at which the POPE/POPG membrane naturally shows coexisting phases. Between 293 and 287 K, the two AMPs clustered and disordered the anionic POPG while ordering the zwitterionic POPE. The cationic peptides most likely partitioned into the disordered phase, which also contains POPE, whose mole fraction depends on the peptide and the temperature. Fig. 7 depicts the membrane domains induced by PG-1 at 293 K, the structure of the peptide and the proposed peptide-lipid interactions in the disordered phase (9,10). If we make the reasonable assumption that the disordered phase also has higher curvature, PG-1 most likely then partitions into the disordered phase because previous lipid-peptide distance measurements indicate that PG-1 is located in the high-curvature toroidal pore defects of the membrane (17).

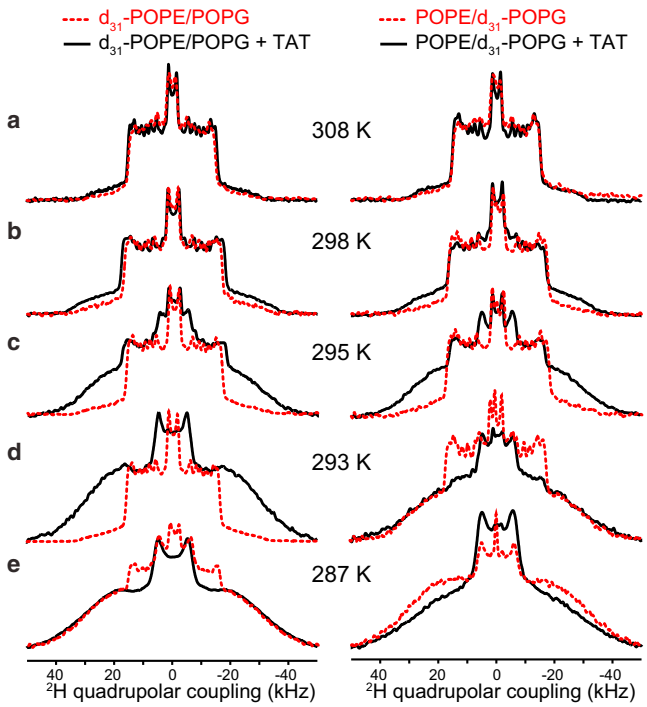

FIGURE 6 Influence of TAT on the disorder of the POPE/POPG membrane, detected from the ^{2}H spectra of d_{31}-POPE (*left column*) and d_{31}-POPG (*right column*) at (*a*) 308 K, (*b*) 298 K, (*c*) 295 K, (*d*) 293 K, and (*e*) 287 K. TAT increases the order of both POPE and POPG between 298 and 287 K. To see this figure in color, go online.

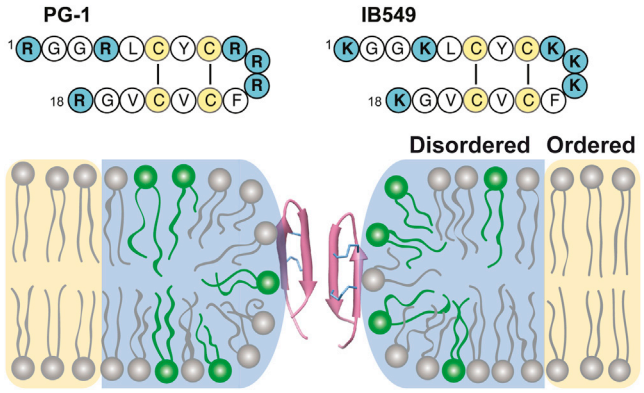

FIGURE 7 Model of PG-1 and IB549-induced lateral domain separation in POPE/POPG (3:1) membranes at ambient temperature. The disordered (LC) and ordered (gel) phases are shaded in blue and yellow, respectively, and POPE and POPG lipids are shown in gray and green, respectively. The numbers of POPG and POPE molecules in the two phases are according to the measured results of PG-1-bound membrane at 293 K. The peptide is most likely associated with the disordered phase because PG-1 has been experimentally shown to bind to toroidal pore defects (17). The amino acid sequences of PG-1 and IB549 are shown at the top. To see this figure in color, go online.

Fig. 7 shows POPE is not exclusively located in the ordered phase but is also present in the disordered phase, which may help to stabilize the curvature of the toroidal pore due to the intrinsic negative curvature of POPE. This lateral domain separation occurs around 293 K for PG-1 and at a slightly higher temperature (~295 K) for IB549. Above these temperatures, the membrane becomes homogeneous, without coexisting LC and gel phases or separate POPE and POPG domains.

These results suggest that the mammalian AMPs studied here, which must act near the physiological temperature of 308 K, do not use domain formation as a significant mechanism against bacterial membranes. However, for AMPs produced by amphibians such as frogs, whose body temperature is mainly controlled by the ambient temperature, the intrinsic ability of POPE and POPG to phase separate at ~293 K may allow these peptides to cluster POPG and induce a separate POPE domain, thus destroying the barrier function of the membranes of Gram-negative bacteria. Further experiments on other AMPs, especially of nonmammalian origin, will be interesting to test this hypothesis. Compared to AMPs, the conformationally flexible HIV TAT exerts little effect on membrane disorder at 308 K, which is consistent with the membrane translocation function of the peptide, but TAT uniformly orders POPE and POPG at lower temperatures, which may reflect the fact that the randomly positioned Arg residues in this unstructured peptide may interact equally well with the phosphate groups of both neutral and anionic lipids.

SUPPORTING MATERIAL

Three figures are available at http://www.biophysj.org/biophysj/supplemental/S0006-3495(13)009333-8.

This work is funded by National Institutes of Health grant GM066976.

We thank Keith Fritzsching for insightful discussions.

REFERENCES

1. Brown, D. A., and E. London. 2000. Structure and function of sphingolipid- and cholesterol-rich membrane rafts. *J. Biol. Chem.* 275:17221–17224.
2. Simons, K., and W. L. C. Vaz. 2004. Model systems, lipid rafts, and cell membranes. *Annu. Rev. Biophys. Biomol. Struct.* 33:269–295.
3. Epand, R. M., and R. F. Epand. 2009. Domains in bacterial membranes and the action of antimicrobial agents. *Mol. Biosyst.* 5:580–587.
4. Epand, R. F., W. L. Maloy, …, R. M. Epand. 2010. Probing the "charge cluster mechanism" in amphipathic helical cationic antimicrobial peptides. *Biochemistry.* 49:4076–4084.
5. Epand, R. F., G. Wang, …, R. M. Epand. 2009. Lipid segregation explains selective toxicity of a series of fragments derived from the human cathelicidin LL-37. *Antimicrob. Agents Chemother.* 53:3705–3714.
6. Epand, R. M., and R. F. Epand. 2009. Lipid domains in bacterial membranes and the action of antimicrobial agents. *Biochim. Biophys. Acta.* 1788:289–294.
7. Mishra, A., V. D. Gordon, …, G. C. L. Wong. 2008. HIV TAT forms pores in membranes by inducing saddle-splay curvature: potential role of bidentate hydrogen bonding. *Angew. Chem. Int. Ed. Engl.* 47: 2986–2989.
8. Schmidt, N. W., A. Mishra, …, G. C. Wong. 2011. Criterion for amino acid composition of defensins and antimicrobial peptides based on geometry of membrane destabilization. *J. Am. Chem. Soc.* 133:6720–6727.
9. Hong, M., and Y. Su. 2011. Structure and dynamics of cationic membrane peptides and proteins: insights from solid-state NMR. *Protein Sci.* 20:641–655.
10. Tang, M., and M. Hong. 2009. Structure and mechanism of beta-hairpin antimicrobial peptides in lipid bilayers from solid-state NMR spectroscopy. *Mol. Biosyst.* 5:317–322.
11. Ganz, T. 2003. Defensins: antimicrobial peptides of innate immunity. *Nat. Rev. Immunol.* 3:710–720.
12. Epand, R. M., and H. J. Vogel. 1999. Diversity of antimicrobial peptides and their mechanisms of action. *Biochim. Biophys. Acta.* 1462:11–28.
13. Fischer, R., M. Fotin-Mleczek, …, R. Brock. 2005. Break on through to the other side-biophysics and cell biology shed light on cell-penetrating peptides. *ChemBioChem.* 6:2126–2142.
14. Su, Y., R. Mani, …, M. Hong. 2008. Reversible sheet-turn conformational change of a cell-penetrating peptide in lipid bilayers studied by solid-state NMR. *J. Mol. Biol.* 381:1133–1144.
15. Su, Y., A. J. Waring, …, M. Hong. 2010. Membrane-bound dynamic structure of an arginine-rich cell-penetrating peptide, the protein transduction domain of HIV TAT, from solid-state NMR. *Biochemistry.* 49:6009–6020.
16. Li, S., Y. Su, …, M. Hong. 2010. Water-protein interactions of an arginine-rich membrane peptide in lipid bilayers investigated by solid-state nuclear magnetic resonance spectroscopy. *J. Phys. Chem. B.* 114:4063–4069.
17. Tang, M., A. J. Waring, and M. Hong. 2007. Phosphate-mediated arginine insertion into lipid membranes and pore formation by a cationic membrane peptide from solid-state NMR. *J. Am. Chem. Soc.* 129:11438–11446.
18. Jang, H., B. Ma, …, R. Nussinov. 2008. Models of toxic beta-sheet channels of protegrin-1 suggest a common subunit organization motif shared with toxic alzheimer beta-amyloid ion channels. *Biophys. J.* 95:4631–4642.
19. Langham, A. A., A. S. Ahmad, and Y. N. Kaznessis. 2008. On the nature of antimicrobial activity: a model for protegrin-1 pores. *J. Am. Chem. Soc.* 130:4338–4346.
20. Mani, R., S. D. Cady, …, M. Hong. 2006. Membrane-dependent oligomeric structure and pore formation of a beta-hairpin antimicrobial peptide in lipid bilayers from solid-state NMR. *Proc. Natl. Acad. Sci. USA.* 103:16242–16247.
21. Mani, R., M. Tang, …, M. Hong. 2006. Membrane-bound dimer structure of a beta-hairpin antimicrobial peptide from rotational-echo double-resonance solid-state NMR. *Biochemistry.* 45:8341–8349.
22. Tang, M., A. J. Waring, …, M. Hong. 2008. Effects of guanidinium-phosphate hydrogen bonding on the membrane-bound structure and activity of an arginine-rich membrane peptide from solid-state NMR spectroscopy. *Angew. Chem. Int. Ed. Engl.* 47:3202–3205.
23. Chen, J., T. J. Falla, …, J. C. Fiddes. 2000. Development of protegrins for the treatment and prevention of oral mucositis: structure-activity relationships of synthetic protegrin analogues. *Biopolymers.* 55:88–98.
24. Hong, M., K. Schmidt-Rohr, and D. Nanz. 1995. Study of phospholipid structure by 1H, 13C, and 31P dipolar couplings from two-dimensional NMR. *Biophys. J.* 69:1939–1950.
25. Hong, M., K. Schmidt-Rohr, and A. Pines. 1995. Measurement of signs and magnitudes of C-H dipolar couplings in lecithin. *J. Am. Chem. Soc.* 117:3310–3311.

26. Bloom, M., J. H. Davis, and A. L. Mackay. 1981. Direct determination of the oriented sample NMR-spectrum from the powder spectrum for systems with local axial symmetry. *Chem. Phys. Lett.* 80:198–202.

27. McCabe, M. A., and S. R. Wassall. 1997. Rapid deconvolution of NMR powder spectra by weighted fast Fourier transformation. *Solid State Nucl. Magn. Reson.* 10:53–61.

28. Pozo Navas, B., K. Lohner, …, G. Pabst. 2005. Composition dependence of vesicle morphology and mixing properties in a bacterial model membrane system. *Biochim. Biophys. Acta.* 1716:40–48.

29. Aussenac, F., M. Laguerre, …, E. J. Dufourc. 2003. Detailed structure and dynamics of bicelle phospholipids using selectively deuterated and perdeuterated labels. H-2 NMR and molecular mechanics study. *Langmuir.* 19:10468–10479.

30. Morse, R. P. D., L. D. Ma, …, F. Dunn. 1999. Ultrasound interaction with large unilamellar vesicles at the phospholipid phase transition: perturbation by phospholipid side chain substitution with deuterium. *Chem. Phys. Lipids.* 103:1–10.

31. Edidin, M. 2003. The state of lipid rafts: from model membranes to cells. *Annu. Rev. Biophys. Biomol. Struct.* 32:257–283.

32. Brown, D. A., and E. London. 1998. Functions of lipid rafts in biological membranes. *Annu. Rev. Cell Dev. Biol.* 14:111–136.

33. Veatch, S. L., I. V. Polozov, …, S. L. Keller. 2004. Liquid domains in vesicles investigated by NMR and fluorescence microscopy. *Biophys. J.* 86:2910–2922.

34. Veatch, S. L., O. Soubias, …, K. Gawrisch. 2007. Critical fluctuations in domain-forming lipid mixtures. *Proc. Natl. Acad. Sci. USA.* 104: 17650–17655.

35. Dolainsky, C., P. Karakatsanis, and T. M. Bayerl. 1997. Lipid domains as obstacles for lateral diffusion in supported bilayers probed at different time and length scales by two-dimensional exchange and field gradient solid state NMR. *Phys. Rev. E.* 55:4512–4521.

36. Lindblom, G., and G. Orädd. 2009. Lipid lateral diffusion and membrane heterogeneity. *Biochim. Biophys. Acta.* 1788:234–244.

37. Su, Y., T. Doherty, …, M. Hong. 2009. Roles of arginine and lysine residues in the translocation of a cell-penetrating peptide from (13)C, (31)P, and (19)F solid-state NMR. *Biochemistry.* 48:4587–4595.

38. Doherty, T., Y. Su, and M. Hong. 2010. High-resolution orientation and depth of insertion of the voltage-sensing S4 helix of a potassium channel in lipid bilayers. *J. Mol. Biol.* 401:642–652.

39. Zhang, Y., W. Lu, and M. Hong. 2010. The membrane-bound structure and topology of a human α-defensin indicate a dimer pore mechanism for membrane disruption. *Biochemistry.* 49:9770–9782.

Supporting Material

A ^{2}H Solid-State NMR Study of Lipid Clustering by Cationic Antimicrobial and Cell-Penetrating Peptides in Model Bacterial Membranes

Byungsu Kwon[1], Alan J. Waring[2], and Mei Hong[1]*

[1] Department of Chemistry, Iowa State University, Ames, Iowa 50011
[2] Department of Physiology and Biophysics, School of Medicine, University of California, Irvine, California 92697-4560 [3] Department of Medicine, Harbor-UCLA Medical Center, Torrance CA 90502

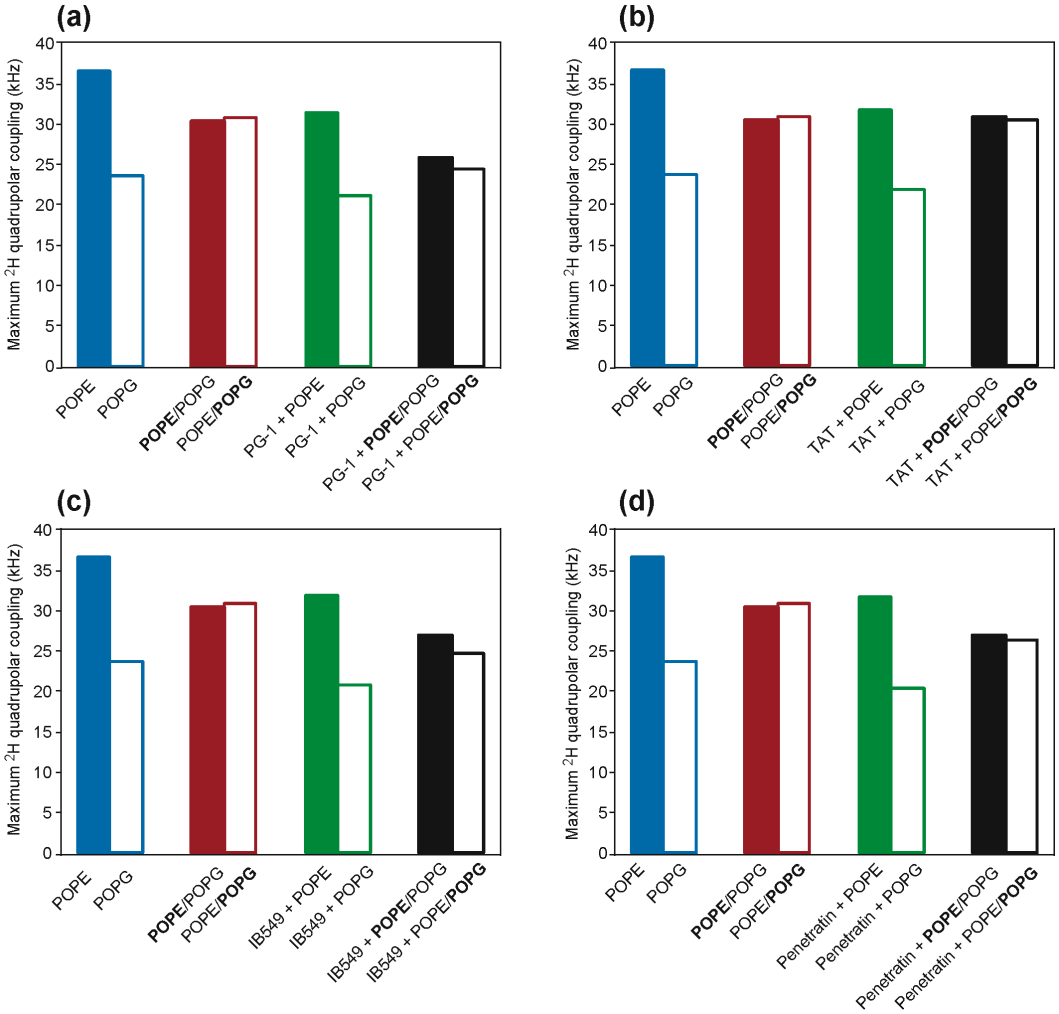

Figure S1. Summary of the maximum ^{2}H quadrupolar couplings of POPE and POPG in various lipid membranes at 308 K. The peptides are (a) PG-1, (b) TAT, (c) IB549, and (d) Penetratin. Filled and open bars represent the couplings of d_{31}-POPE and d_{31}-POPG, respectively.

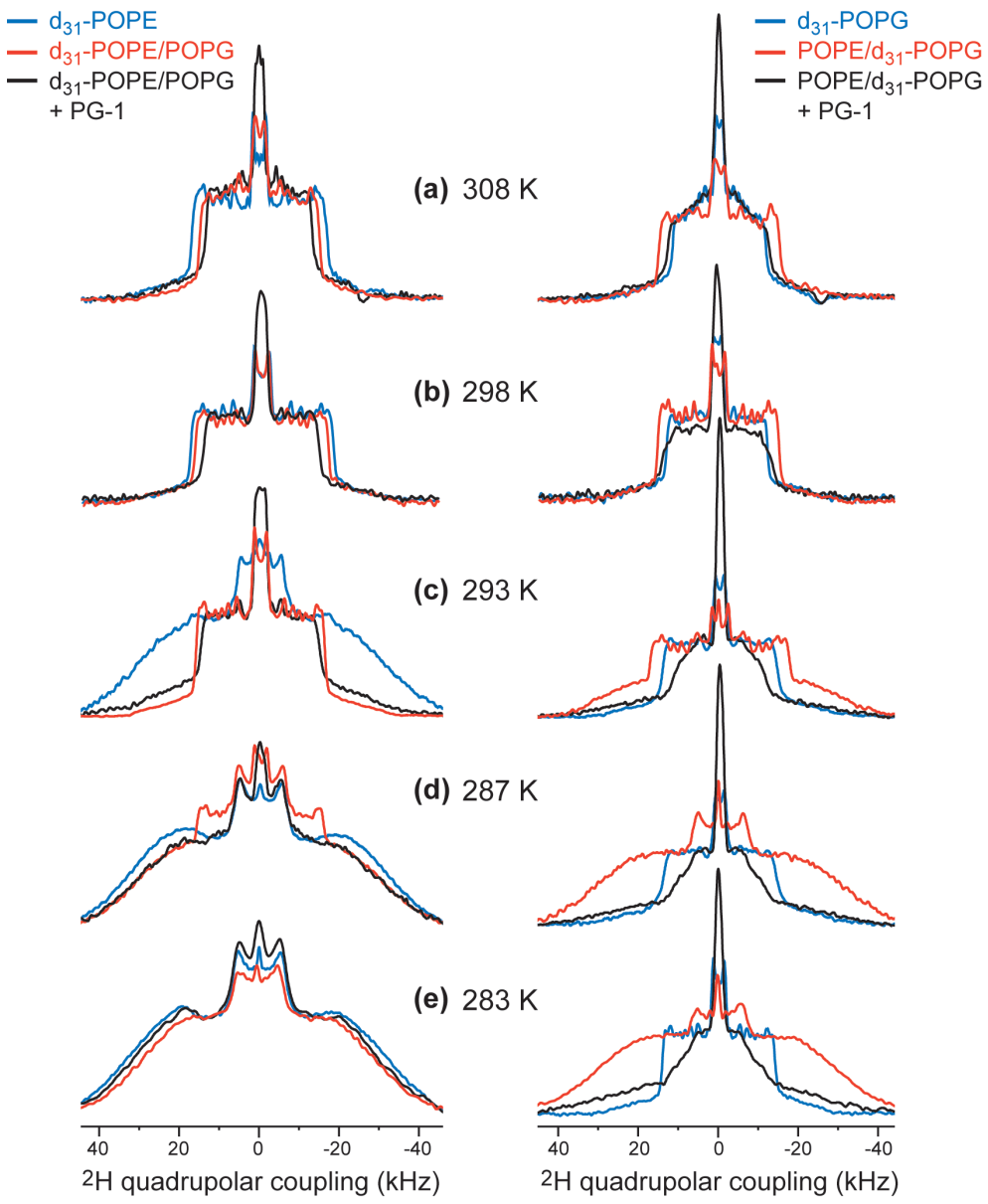

Figure S2. ^{2}H spectra of d_{31}-POPE (left column) and d_{31}-POPG (right column) in lipid membranes without and with PG-1 from 308 K to 283 K. In each panel, the spectra of pure POPE or POPG membrane, the peptide-free POPE/POPG membrane, and the peptide-bound POPE/POPG membrane are superimposed.

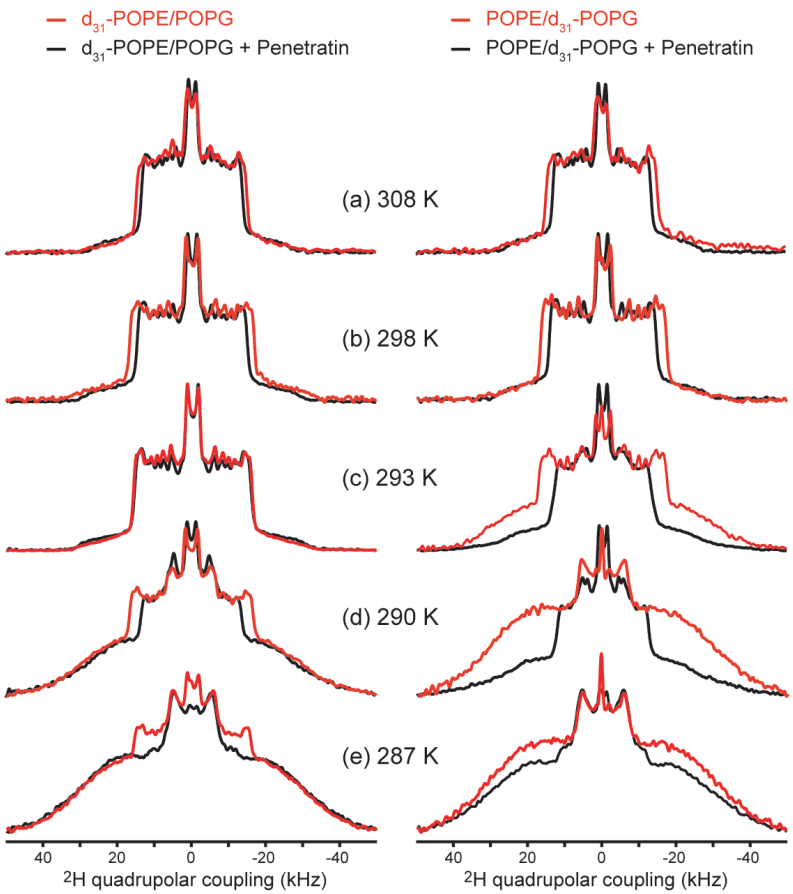

Figure S3. Influence of penetratin on the POPE/POPG membrane disorder, as detected from the ^{2}H spectra of d_{31}-POPE (left column) and d_{31}-POPG (right column) at (a) 308 K, (b) 298 K, (c) 293 K, (d) 290 K, and (d) 287 K. Penetratin retained or increased the order of POPE while decreasing the order of POPG between 293 K and 287 K.